Journal of Pain Research

Dovepress
Taylor & Francis Group

Open Access Full Text Article

CLINICAL TRIAL REPORT

Tuina Alleviates Pain Associated with Lumbar Disc Herniation by Regulating Functional Connectivity Between Inferior Frontal Triangularis and Multiple Brain Networks: A Randomized Controlled fMRI Study

Changzheng Jiang[1,*], Huanzhen Zhang[2,3,*], Xiaoyan Wu[4,*], Lanting Huang[1], Xuekun Zhou[1], Jian Lin[2,3], Lechun Chen[2,3], Hongye Huang[2,3], Shuijin Chen[2,3], Jinkun Zhang[4], Zhigang Lin[2,3]

[1]Acupuncture and Moxibustion Tuina College, Fujian University of Traditional Chinese Medicine, Fuzhou, Fujian, People's Republic of China; [2]Department of Tuina, Rehabilitation Hospital Affiliated to Fujian University of Traditional Chinese Medicine, Fuzhou, Fujian, People's Republic of China; [3]Fujian Key Laboratory of Rehabilitation Technology, Fuzhou, Fujian, People's Republic of China; [4]School of Psychology, Fujian Normal University, Fuzhou, Fujian, People's Republic of China

*These authors contributed equally to this work

Correspondence: Jinkun Zhang, School of Psychology, Fujian Normal University, Fuzhou, Fujian, People's Republic of China, Email jinkunzhang@126.com; Zhigang Lin, Department of Tuina, Rehabilitation Hospital affiliated to Fujian University of Traditional Chinese Medicine, Fuzhou, Fujian, People's Republic of China, Email drlzg2014@126.com

Purpose: This study conducted a randomized controlled trial by analyzing resting-state functional magnetic resonance imaging (rs-fMRI) data to determine the mechanisms by which Tuina alleviates pain and modulates multiple brain networks in lumbar disc herniation (LDH) patients.

Patients and Methods: This study included 38 healthy subjects and 76 LDH patients. LDH patients were randomly assigned into the test group (TG; n = 38) and control group (CG; n = 38). TG patients received 14 days of Tuina therapy, whereas CG patients received a combination of transcutaneous electrical nerve stimulation (TENS) and lumbar traction therapy. The primary outcome measure, simplified McGill Pain Questionnaire (SF-MPQ), was used to assess pain. Pain pressure threshold (PPT), Oswestry Disability Index (ODI), Beck Depression Inventory II (BDI-II), and Beck Anxiety Inventory (BAI) were evaluated as secondary outcomes. Fractional amplitude of low-frequency fluctuation (fALFF) and functional connectivity (FC) values were evaluated from the rs-fMRI data before and after treatment.

Results: The SF-MPQ score significantly decreased in both TG subjects [−13.00 (−19.00, −9.00); P <0.001] and CG subjects [−11.00 (−14.00, −7.00); P <0.001]. SF-MPQ scores were significantly different between the two groups (P <0.05). In TG subjects, Tuina inhibited spontaneous neural activity in the bilateral inferior frontal gyrus triangular part (IFGtri) and suppressed the interaction between IFGtri and other brain regions. Changes in FC between IFGtri.R and STG.pole.R positively correlated with improvements in SF-MPQ scores (r = 0.511, P = 0.005). Changes in FC between IFGtri.L and IFGtri.R negatively correlated with reduced PPT of the bilateral gluteus maximus (r = −0.518, P = 0.004).

Conclusion: Tuina effectively alleviates pain, lumbar dysfunction, and negative emotions in LDH patients by regulating the interactions between multiple neural networks in the brain, especially through the inferior frontal gyrus triangle area.

Keywords: lumbar disc herniation, functional magnetic resonance imaging, analgesia, Tuina, resting-state, inferior frontal gyrus triangle area

Introduction

Lumbar disc herniation (LDH) is a degenerative disorder in which the nucleus pulposus, a gel-like substance at the center of the lumbar disc, extends through a rupture in the annulus fibrosus, the surrounding fibrous ring.[1] This causes

https://doi.org/10.2147/JPR.S592723
Received: 30 December 2025
Accepted: 4 March 2026
Published: 12 March 2026

Graphical Abstract

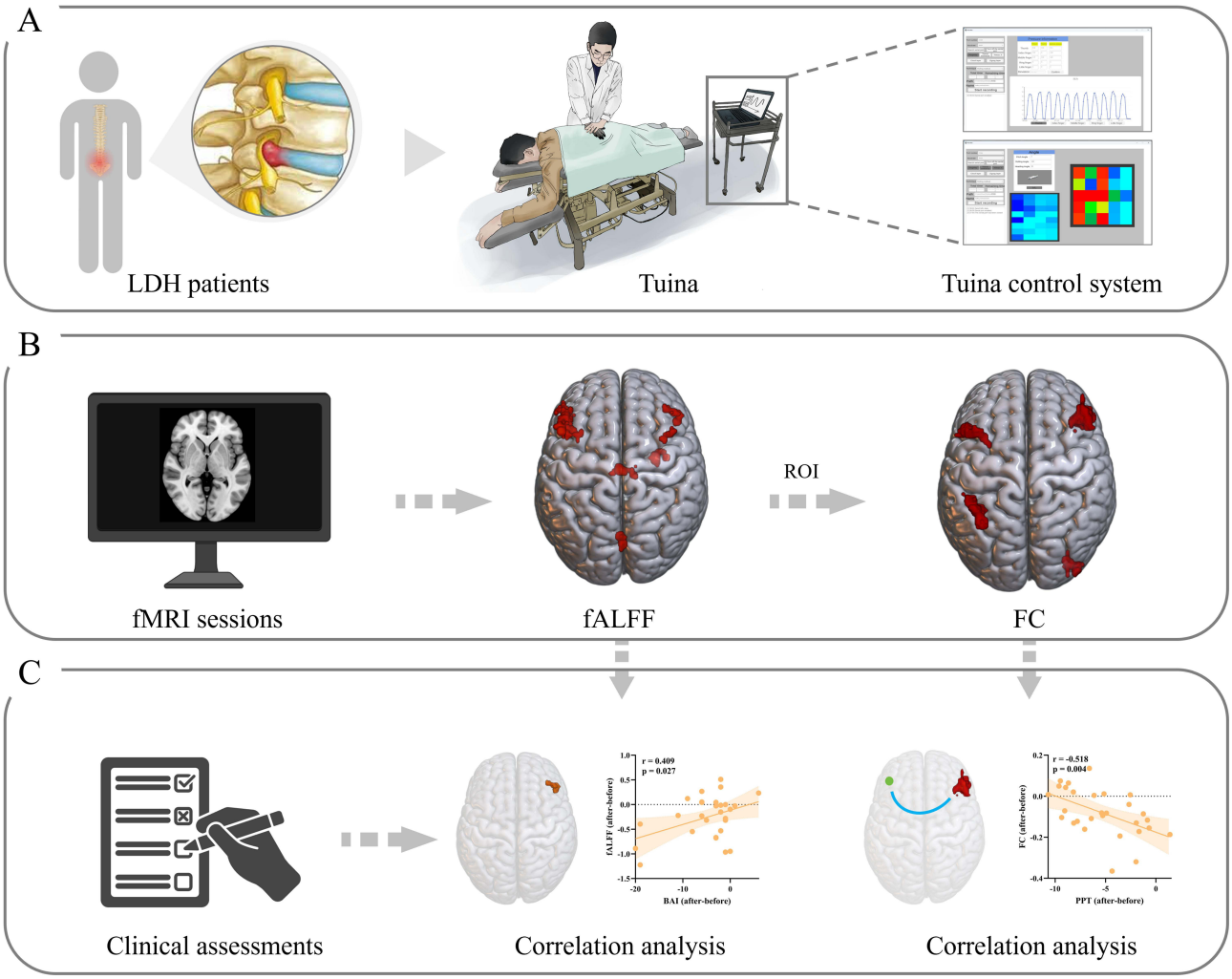

mechanical compression and inflammation of the nearby nerve roots and dura mater, leading to clinical symptoms such as low back pain, radiating leg pain, and functional impairments.[2] LDH is a significant public health concern worldwide.[3] Epidemiological data shows that the number of LDH cases is rising annually and its prevalence is increasing significantly among the younger population. In the United States, back pain represents the largest category of healthcare spending with an estimated annual expenditure of 134.5 billion dollars.[4] LDH patients suffer from prolonged and recurrent symptoms.[5,6] Long-term reliance on opioid medications is complicated because it can lead heart and kidney dysfunctions, adverse gastrointestinal effects, and drug dependency.[7,8] Consequently, there is an urgent need to understand the underlying pathological mechanisms for developing safe and effective non-pharmacological therapies.

The pain mechanism of LDH is highly complex and involves both the central nervous system (CNS) and the peripheral nervous system (PNS). CNS becomes hypersensitive to pain because of persistent peripheral nociceptive signals that are transmitted to the brain through the dorsal horn of the spinal cord. This initiates the "central sensitization" process, which involves reorganization of the brain networks and imbalanced emotional regulation, leading to amplification and sustenance of pain signals.[9–11] Resting-state functional magnetic resonance imaging (rs-fMRI) studies have revealed abnormal activity in the medial prefrontal cortex and sensory-motor cortex of patients with LDH.[12] Furthermore, LDH leads to significant changes in the functional connectivity (FC) of brain regions associated with the

visual network.[13] Therefore, CNS mechanisms play a pivotal role in the chronic progression of LDH, contributing to persistent pain, lumbar dysfunction, and negative emotional states.

Tuina is a form of therapeutic massage based on the principles of traditional Chinese medicine (TCM) and involves mechanical manipulation of the body's meridians, acupoints, and joints to restore balance between yin and yang, facilitating disease recovery. Previous researches have shown that Tuina is effective in alleviating pain and reducing negative emotions in individuals with chronic conditions.[14,15] A systematic review found moderate evidence supporting the efficacy of Tuina in alleviating adult pain.[16] Despite its widespread use in clinical practice for musculoskeletal problems and other conditions, the efficacy of Tuina is controversial. Therefore, clinical application of Tuina requires understanding the mechanisms by which it regulates dynamic brain function to relieve pain.

Functional magnetic resonance imaging (fMRI) is a non-invasive neuroimaging method to visualize and understand the effects of Tuina on the CNS.[17,18] Previous fMRI studies have shown that Tuina modulates pain-related brain regions such as thalamus, anterior cingulate gyrus, parietal lobe, and primary somatosensory cortex. Song et al[19] performed rs-fMRI data analysis of patients with painful cervical spondylosis and reported that Tuina alleviates neck pain by modulating activity in the pain-associated brain regions. Zhou et al[20] found that Tuina relieves pain in LDH patients by adjusting the functional connectivity (FC) between the default mode network and the dorsal attention network. Chen et al[21] reported that Tuina reshapes the default mode network and strengthens the internal FC. However, these studies focused only on the default mode network and did not analyze other important regions of the brain. Moreover, these studies did not include intervention control groups. Therefore, it was difficult to determine the effects of time or different interventions.

This randomized controlled trial analyzed resting-state fMRI data to investigate the effects of Tuina on the spontaneous neural activity and brain networks of LDH patients by evaluating voxel-based fractional amplitude of low-frequency fluctuation (fALFF) and seed-based FC. Correlation analysis was conducted to evaluate the relationship between changes in fALFF and FC before and after treatment and the clinical outcome measures.

Methods

This study included 76 LDH patients and 38 healthy participants. The sample size was calculated using G*Power 3.1 (http://www.gpower.hhu.de/) to account for a 20% dropout rate.[21,22] The study protocol was approved by the Ethics Review Committee of the Rehabilitation Hospital Affiliated of Fujian University of Traditional Chinese Medicine (Ethical Approval No: 2024KY-008-02) and was registered with the Chinese Clinical Trial Registry (Registration No: ChiCTR2400083784). The detailed protocol was performed as previously reported.[23]

Study Design

We screened 163 patients between May 2024 and December 2024 from the Tuina Department of the Rehabilitation Hospital Affiliated of Fujian University of Traditional Chinese Medicine and the WeChat account of the hospital and included 76 eligible LDH patients and 38 healthy participants who were matched for age, gender, and education. LDH patients were randomly assigned to either the test group (TG) or control group (CG) (n = 38 each). The 38 healthy participants were assigned to the healthy group (HG). Since four participants withdrew, the final analysis included 35 patients in the TG and 37 in the CG (Figure 1). The persons responsible for outcome measurement, data collection, and analyses were performed independently by three researchers who were blinded to the group allocation. The study schedule is shown in Figure 2.

Inclusion and Exclusion Criteria

The inclusion criteria for healthy participants were as follows: (1) right-handed; (2) aged 18–60 years; (3) no history of LDH; (4) no pain history related to any disease in the past month and no pain treatments; (5) Beck Depression Inventory-II (BDI-II) score ≤13; (6) Beck Anxiety Inventory (BAI) score <45; (7) voluntary consent to participate and signed the informed consent form.

The inclusion criteria for LDH patients[24] were as follows: (1) right-handed; (2) aged 18–60 years; (3) prior CT or MRI showed L4-L5 and/or L5-S1 disc herniation; (4) predominant radicular pain, with imaging-confirmed disc

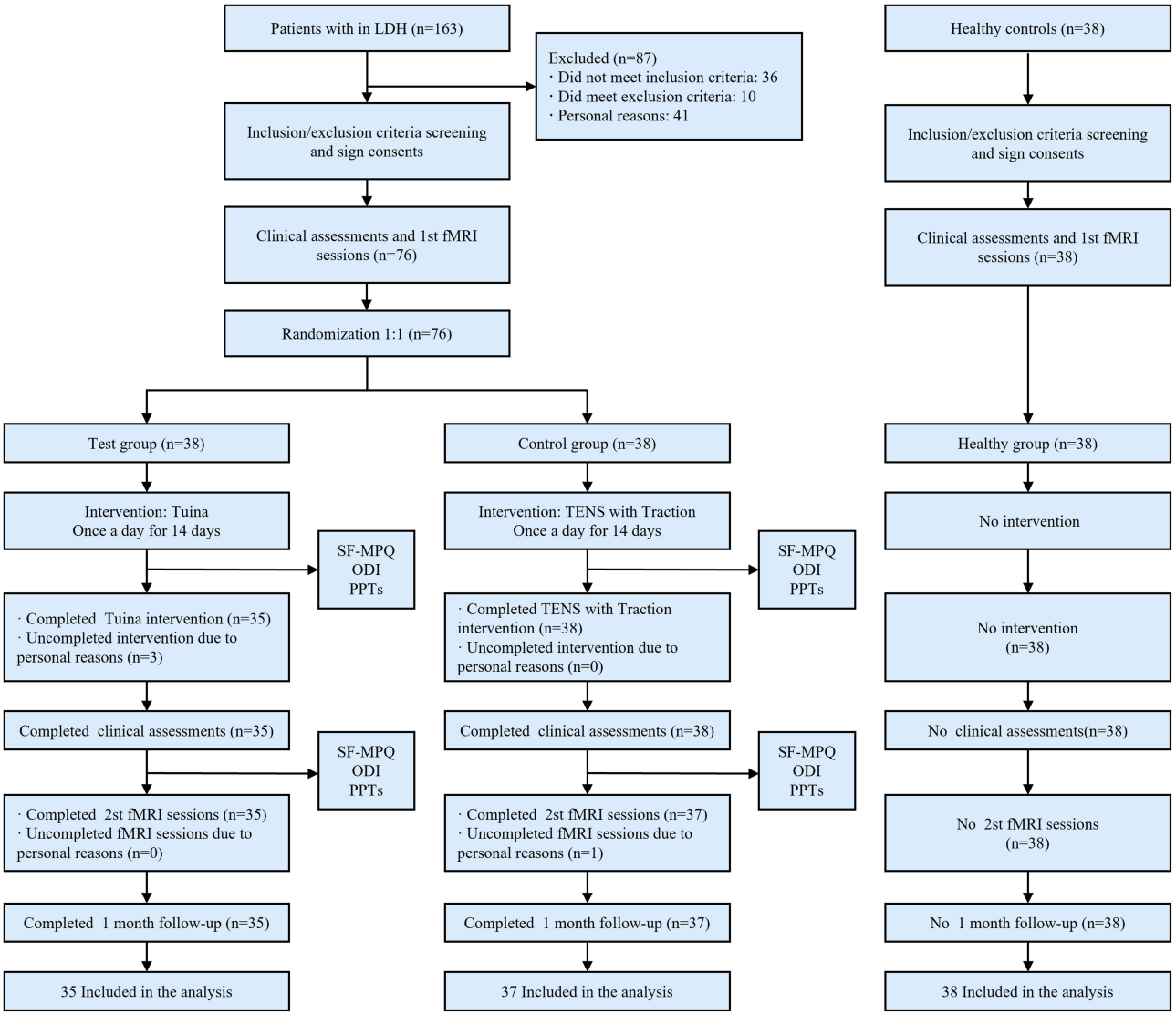

Figure 1 Flowchart of study strategy.

herniation matching the neurological level; (5) Douleur Neuropathique 4 questions (DN4) score ≥4, Visual Analog Scale (VAS) score ≥3 and ≤8; (6) lumbar and leg pain symptoms lasting ≥3 months; (7) no use of pain relief or neurotrophic medications in the last month and no systemic treatments; (8) voluntary consent to participate and provided written informed consent. Exclusion criteria for LDH patients were as follows: (1) significant nucleus pulposus protrusion compressing the spinal cord or cauda equina with progressive neurological dysfunction; (2) coexisting lumbar spondylolysis or moderate-to-severe spondylolisthesis; (3) other serious lumbar diseases such as tumors, tuberculosis, or severe osteoporosis; (4) acute lumbar injury pain or lower limb nerve damage due to trauma or surgery; (5) conditions causing lower limb neuropathy; (6) significant comorbidities such as cardiovascular, pulmonary, renal, or hematological disorders; (7) psychiatric disorders; (8) pregnant or breastfeeding women; (9) contraindications for MRI.

Interventions

LDH participants were treated daily for 14 days. The test group (TG) patients received treatment from a professionally trained Tuina therapist. The control group (CG) patients underwent transcutaneous electrical nerve stimulation (TENS) and lumbar traction conducted by a senior physical therapist. Medication, acupuncture, and other physical therapies were not allowed during the treatment period.

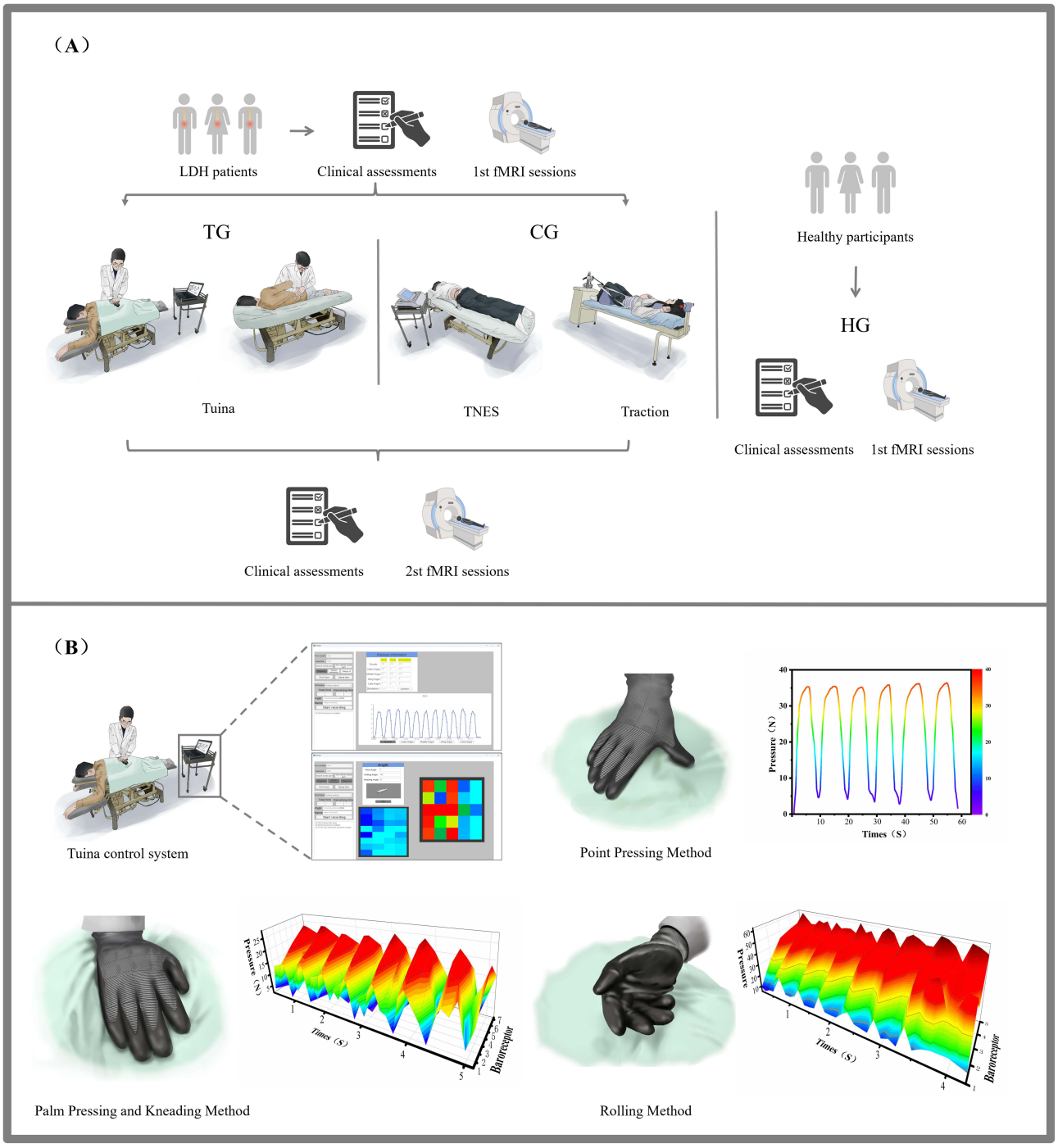

Figure 2 Experimental design and Tuina control.
Notes: (**A**) Experimental design. (**B**) Tuina control progress.
Abbreviations: TG, test group; CG, control group; HG, healthy group; TNES, transcutaneous electrical nerve stimulation.

Test Group

Tuina therapy was performed according to previously established TCM principles and methodology.[25] The specific treatment steps are described below (Figure 2). Step 1: The Tuina therapist guided the patient into a prone position and applied pressure and rubbing along the bladder meridian on the patient's lower back, hips, and posterior lateral side of the affected leg for 10 minutes. Step 2: The therapist rhythmically pressed the acupoints of the affected side, including Shenshu point (BL23), Dachangshu point (BL25), Huantiao point (GB30), Chengfu point (BL36), Weizhong point

https://doi.org/10.2147/JPR.S592723

(BL40), Chengshan point (BL57), and Kunlun point (BL60), using the thumb for 10 minutes. Step 3: The therapist performed rolling (up and down) motion on the patient's lower back and hips for 5 minutes. Step 4: After guiding the patient to lay on the side, the therapist performed the lateral pull technique at the waist once on each side. Step 5: The patient was guided to lay on the back. Then, the therapist lifted the affected leg in a procedure like the straight leg raise test and repeated it several times.

During the Tuina procedure, the therapist used a smart Tuina glove developed by our team to precisely quantify the technique parameters. The glove integrates mechanical and sensor-based principles and features multi-point flexible pressure sensors on the threaded surface of each finger as well as the thenar and hypothenar regions for three-dimensional pressure sensing. This allowed real-time sampling of force and frequency. The glove also contained a three-axis accelerometer and gyroscope to measure direction and angle. The wrist area of the glove was equipped with a data acquisition board to process sensor data and transmit it to a PC-based visualization interface. The therapist could adjust the technique by reviewing real-time data, graphical trends, and analysis results to ensure accuracy (see Figure 2). The specific parameters[26] are described below.

Palm Pressing and Kneading Method

Using elbow as a pivot, the right palm's base applied pressure aided by the left palm at the back of the right palm. The forearm actively performed small circular kneading movements of the wrist and palm. This combination of pressing and kneading was applied rhythmically to the subcutaneous tissues at a frequency of 80 times per minute and a force of 15–25N.

Point Pressing Method

Using right wrist as the pivot, the right thumb tip applied rhythmic pressure to the acupoints at a frequency of 10 times per minute with a force of 30–40 N.

Rolling Method

Using elbow as the pivot, the dorsal side of the little finger's metacarpophalangeal joint acted as the main pressure point to the affected area and performed rhythmic rolls back and forth at a frequency of 120 times per minute with a force of 40–60 N.

Control Group

Step 1: The patient lay prone on the treatment table. The therapist placed two electrodes from the TENS device (WOND2000F0, SUNJAVA) on the patient's lower back and legs at the "Ah Shi" acupoints. The frequency was adjusted to 25 Hz and a pulse width of 280 μs. The intensity was set according to the patient's condition and tolerance. The treatment time was 20 minutes. Step 2: Lumbar traction was administered after 10 minutes of TENS. The patient was positioned on a spinal traction bed (TC-30S, MINATO). After assisting the patient with the traction belt, the initial traction force was set at 25% of the patient's weight and gradually increased in 2 kg increments until the force reached 40–50% of their weight. The duration of traction was 20 minutes. After each session, the patient was required to lie flat and rest for 5 minutes.

Clinical Assessment

In this trial, the primary outcome measure was the simplified McGill Pain Questionnaire (SF-MPQ),[27] which assessed pain rating index (PRI), VAS, and present pain intensity (PPI) as the three pain-related indicators. Pain pressure threshold (PPT), Oswestry Disability Index (ODI),[28] BDI-II[29] and BAI[30] were used as secondary outcome measures to assess the soft tissue pain threshold, lumbar function, as well as depression and anxiety levels of the patient.

fMRI Data Acquisition

fMRI was conducted using a Siemens MAGNETOM Prisma 3.0T MRI scanner. To minimize noise interference and reduce head movement during scanning, participants wore earplugs and a sponge pad. They were instructed to close their

eyes, relax, stay awake, maintain a fixed head position, and avoid mental activity. In case of discomfort, participants could press an alarm to signal the staff to halt the scan. The acquisition parameters for T1-weighted 3D magnetization-prepared rapid gradient-echo (MP-RAGE) sequence were as follows: repetition time (TR) = 2200 ms, echo time (TE) = 2.48 ms, flip angle (FA) = 8°, field of view (FOV) = 230 mm × 230 mm, matrix = 256 × 256, resolution = 0.98 × 0.98 × 1 mm^3, and slice count = 160, slice thickness = 1.0 mm, scan duration = 338 seconds.[23] fMRI images with a gradient-echo echo-planar imaging (GE-EPI) sequence were acquired across 300 time points using the following parameters: TR = 2000 ms, TE = 30 ms, FA = 90°, FOV = 230 mm × 230 mm, Matrix = 64 × 64, Resolution = 3.6 × 3.6 × 3.6 mm^3, Number of slices = 37, Slice thickness = 3.6 mm, scan duration = 608 seconds.

Data Analysis

Clinical Data Analysis

All clinical data was analyzed using the SPSS 26.0 software. Normality was tested using the Shapiro–Wilk test and a Quantile–Quantile Plot (Q–Q plot) analysis. Parametric tests were used for normally distributed data and non-parametric tests were used for non-normally distributed data. Statistical analyses were performed using the Chi-squared test, Kruskal–Wallis *H*-test, Mann–Whitney *U*-test, Kruskal–Wallis One-Way ANOVA test, paired *t*-test between groups, Wilcoxon test between groups, and two-sample tests. $P < 0.05$ was considered statistically significant.

fMRI Data Analysis

The fMRI data was preprocessed using the SPM 12 software (https://www.fil.ion.ucl.ac.uk/spm/software/spm12/) on the MATLAB platform and the DPABI v8.0 toolbox (http://www.rfmri.org/). The first 10 functional images were discarded because of adaptation and signal stabilization issues. Temporal slice correction was performed using slice 37 as the reference. Head motion correction was applied and subjects with translations >2 mm or rotations >2° were excluded from the analysis. Mean framewise displacement (FD) was calculated using the Jenkinson model to ensure no significant group effects ($P > 0.05$).[31]

Structural images were co-registered with functional images and segmented into white matter, gray matter, and cerebrospinal fluid. Covariates like the Friston 24 head motion parameters and the average signals from the white matter and cerebrospinal fluid were included in the regression analysis to reduce noise. Functional images were spatially normalized to MNI-152 space with voxel resampling at 3 × 3 × 3 mm^3. Spatial smoothing with a Gaussian kernel (FWHM = 4 mm) and bandpass filtering (0.01–0.1 Hz) was performing to reduce high-frequency noise.[32,33]

fALFF was used to measure spontaneous brain activity. The fast Fourier transform (FFT) was applied to convert the time series of each voxel into the frequency domain. The fALFF value was estimated as ratio of the low-frequency power (0.01–0.1 Hz) to total power and converted into z-scores for statistical analysis.

For the seed-based FC analysis, a brain region displaying spontaneous activity changes was chosen as the seed. This region was defined as a 5 mm radius sphere centered at the peak of the identified area. Subsequently, the mean time-series was extracted for all voxels within the defined seed region for each subject. The Pearson correlation coefficient was then calculated between the seed's time series and all the voxels in the brain to generate a FC map, which was then subjected to Fisher's z-transformation to improve normality for statistical analysis.

Statistical analysis of the initial MRI data was used to compare the brain functional metrics between LDH patients and the healthy control subjects. Imaging data from 6 HG, 3 TG, and 2 CG participants was excluded because of excessive motion or failed spatial normalization. A two-sample *t*-test was used to compare the difference in the fALFF and FC values between 71 LDH patients and 32 HG participants, as well as between the TG (n = 35) and CG (n = 36) participants.

Voxel-wise two-way repeated-measure ANOVA (group [TG and CG]xtime [pre- and post-intervention]) was conducted on fALFF and FC maps to assess neuroimaging differences between the TG and CG groups.[33] Data of participants with excessive head motion or failed normalization at either time point was excluded. The final analysis included 29 TG and 33 CG participants. Statistical maps were corrected for multiple comparisons using the Gaussian Random Field correction method (voxel-level $P < 0.01$, cluster-level $P < 0.05$). For regions showing significant group × time interactions, mean values were extracted for further analysis ($P < 0.05$). Based on exploratory research, Pearson's

correlation analysis was used to evaluate the relationship of changes in fALFF or FC with the clinical indicators ($P < 0.05$).

Results

Baseline Demographic and Clinical Characteristics

There were no statistically significant differences in gender, age, BMI, or education level between the CG, TG, and HG subjects ($P > 0.05$). Furthermore, there were no significant differences in the dietary preferences, medication willingness, pain location, disease duration, or DN4 between the TG and CG subjects ($P > 0.05$) (Table 1). Since the baseline

Table 1 Baseline Demographic and Clinical Characteristics of the Participants

Items	Test Group (n=35)	Control Group (n=37)	Healthy Group (n=38)	X^2/H/Z value	p-value
Female n (%)	15 (42.86)	20 (54.05)	16 (42.11)	1.330[a]	0.514[a]
Age M (P25, P75), y	37.00 (30.00, 48.00)	39.00 (34.50, 44.50)	37.50 (29.75, 46.50)	0.873[b]	0.646[b]
BMI M (P25, P75), kg/m2	22.50 (20.70, 25.60)	23.50 (22.20, 27.70)	23.18 (21.62, 25.41)	2.751[b]	0.253[b]
Education n (%)					
Primary School and below	3 (8.57)	2 (5.41)	3 (7.89)	0.322[b]	0.851[b]
Junior High School	2 (5.71)	3 (8.11)	1 (2.63)		
High or Technical Secondary School	3 (8.57)	1 (2.70)	4 (10.53)		
Junior College	5 (14.29)	6 (16.22)	3 (7.89)		
Undergraduate	16 (45.71)	20 (54.05)	20 (52.63)		
Graduate student and above	6 (17.14)	5 (13.51)	7 (18.42)		
Dietary preferences n (%)					
Smoking	4 (11.43)	6 (16.22)	6 (15.79)	0.404[a]	0.817[a]
Alcohol consumption	0 (0.00)	0 (0.00)	1 (2.63)	1.912[a]	0.384[a]
Strong tea or coffee	6 (17.14)	10 (27.02)	7 (18.42)	1.280[a]	0.527[a]
Willingness to take medicine n (%)	8 (22.86)	7 (18.92)	–	0.169[a]	0.681[a]
Site of left leg pain or discomfort n (%)	19 (54.29)	16 (43.24)	–	0.878[a]	0.349[a]
Duration of illness M (P25, P75), y	4.00 (1.00, 10.00)	3.00 (1.00, 8.00)	–	−0.979[c]	0.328[c]
DN4 M (P25, P75)	4.00 (4.00, 5.00)	4.00 (4.00, 5.00)	–	−0.614[c]	0.539[c]
SF-MPQ M (P25, P75)	21.00 (16.00, 25.00)	18.00 (14.50, 24.00)	–	−1.151[c]	0.250[c]
PRI	13.00 (9.00, 16.00)	11.00 (9.00, 15.00)	–	−0.972[c]	0.331[c]
VAS	6.00 (4.00, 7.00)	5.00 (4.00, 6.00)	–	−0.946[c]	0.344[c]
PPI	2.00 (1.00, 3.00)	2.00 (2.00, 3.00)	–	−0.042[c]	0.967[c]
ODI M (P25, P75), %	22.00 (18.00, 36.00)	26.00 (18.00, 34.00)	–	−0.384[c]	0.701[c]
Healthy side minus the patient's PPTs M (P25, P75), bf					
Erector spinae muscles	5.24 (3.50, 7.46)	4.86 (4.13, 6.48)	–	−0.186[c]	0.853[c]
Gluteus maximus muscles	5.82(3.26, 9.00)	5.02 (3.38, 7.48)	–	−0.383[c]	0.702[c]
BDI-II M (P25, P75)	9.00 (4.00, 10.00)	9.00 (3.00, 13.50)	1.00 (0.00, 7.25)	14.399[b]	0.001[b] 1.000[T-C] 0.010[T-H] 0.001[C-H]
BAI M (P25, P75)	32.00 (27.00, 36.00)	30.00 (28.00, 36.00)	26.00 (24.00, 29.00)	23.379[b]	0.000[b] 1.000[T-C] 0.000[T-H] 0.000[C-H]

Notes: [a]Denotes p-value representing the X^2 value from the Chi-square analysis; [b] denotes p-value representing the H value from the Kruskal–Wallis test; [c] p-value representing the Z value from the Mann–Whitney *U*-test; [T-C] p-value from the Kruskal–Wallis One-Way ANOVA test comparing the test and control groups; [T-H] p-value obtained from the Kruskal–Wallis One-Way ANOVA test comparing the test and healthy groups; [C-H] p-value from the Kruskal–Wallis One-Way ANOVA test comparing the control and healthy groups.

Abbreviations: M, median; P25, 25th percentile; P75, 75th percentile; DN4, Douleur Neuropathique 4; SF-MPQ, Simplified McGill Pain Questionnaire; PRI, Pain Rating Index; VAS, Visual Analog Scale; PPI, Present Pain Intensity; ODI, Oswestry Disability Index; PPT, Pain Pressure Threshold; BDI-II, Beck Depression Inventory-II; BAI, Beck Anxiety Inventory.

characteristics of the three groups were not normally distributed, statistical data is presented as the median (upper quartile, lower quartile).

Clinical Outcome Measures

The clinical results for the TG and CG subjects are shown in Table 2 and Figure 3. We evaluated the differences in the SF-MPQ, PPT, ODI, BDI-II, and BAI parameters between the two groups on days 1, 7, 10, and 14 of treatment, as well as

Table 2 Clinical Outcomes During the Study

Items	Test Group (n=35)	Control Group (n=37)	p-value
SF-MPQ M (P25, P75)			
Baseline	21.00 (16.00, 25.00)	18.00 (14.50, 24.00)	0.250[c]
1st treatment	16.00 (12.00, 20.00)	13.00 (11.00, 16.50)	0.060[c]
7st treatment	11.00 (7.00, 15.00)	10.00 (6.50, 12.00)	0.139[c]
10st treatment	9.00 (6.00, 12.00)	8.00 (5.00, 12.00)	0.639[c]
14st treatment	6.00 (4.00, 9.00)	6.00 (5.00, 10.00)	0.288[c]
1st month after treatment	6.00 (4.00, 11.00)	8.00 (3.50, 10.00)	0.473[c]
14st treatment-baseline	−13.00 (−19.00, −9.00)	−11.00 (−14.00, −7.00)	0.044[c]
p*	<0.001[d]	<0.001[e]	
PRI M (P25, P75)			
Baseline	13.00 (9.00, 16.00)	11.00 (9.00, 15.00)	0.331[c]
1st treatment	9.00 (6.00, 11.00)	7.00 (5.50, 10.00)	0.240[c]
7st treatment	5.00 (3.00, 9.00)	4.00 (2.50, 6.00)	0.163[c]
10st treatment	5.00 (3.00, 6.00)	4.00 (2.00, 6.00)	0.206[c]
14st treatment	3.00 (2.00, 4.00)	4.00 (2.00, 5.00)	0.299[c]
1st month after treatment	2.00 (2.00, 6.00)	3.00 (1.00, 5.00)	0.860[c]
14st treatment-baseline	−9.00 (−13.00, −6.00)	−7.00(−10.50, −5.50)	0.137[c]
p*	<0.001[d]	<0.001[e]	
VAS score M (P25, P75)			
Baseline	6.00 (4.00, 7.00)	5.00 (4.00, 6.50)	0.320[c]
1st treatment	5.00 (3.00, 6.00)	5.00 (4.00, 6.00)	0.309[c]
7st treatment	3.00 (2.00, 5.00)	4.00 (3.00, 5.00)	0.502[c]
10st treatment	3.00 (2.00, 4.00)	3.00 (2.00, 5.00)	0.310[c]
14st treatment	2.00 (1.00, 3.00)	3.00 (2.00, 4.00)	0.238[c]
1st month after treatment	2.00 (1.00, 3.00)	3.00 (2.00, 4.50)	0.026[c]
14st treatment-baseline	−3.00 (−5.00, −2.00)	−2.00 (−3.00, −1.00)	0.035[c]
p*	<0.001[d]	<0.001[e]	
PPI M (P25, P75)			
Baseline	2.00 (1.00, 3.00)	2.00 (2.00, 3.00)	0.976[c]
1st treatment	2.00 (1.00, 3.00)	1.00 (1.00, 2.00)	0.001[c]
7st treatment	1.00 (1.00, 2.00)	1.00 (1.00, 1.00)	0.001[c]
10st treatment	1.00 (1.00, 1.00)	1.00 (1.00, 1.00)	0.382[c]
14st treatment	1.00 (1.00, 1.00)	1.00 (1.00, 1.00)	0.629[c]
1st month after treatment	1.00 (0.00, 1.00)	1.00 (1.00, 1.00)	0.934[c]
14st treatment-baseline	−1.00 (−2.00, −1.00)	−1.00 (−2.00, −1.00)	0.696[c]
p*	<0.001[e]	<0.001[e]	

(*Continued*)

https://doi.org/10.2147/JPR.S592723

Table 2 (Continued).

Items	Test Group (n=35)	Control Group (n=37)	p-value
ODI M (P25, P75), %			
Baseline	22.00 (18.00, 36.00)	26.00 (18.00, 34.00)	0.701[c]
1st treatment	22.00 (16.00, 34.00)	23.40 (18.00, 29.40)	0.933[c]
7st treatment	16.00 (12.00, 24.00)	20.00 (12.30, 27.00)	0.187[c]
10st treatment	12.00 (7.20, 16.20)	20.00 (13.00, 24.00)	0.002[c]
14st treatment	6.00 (4.00, 14.00)	16.00 (10.50, 24.00)	0.001[c]
1st month after treatment	6.00 (2.00, 12.00)	16.00 (9.50, 27.00)	0.000[c]
14st treatment-baseline	−17.60 (−27.00, −12.00)	−6.00 (−15.00, −2.00)	0.000[c]
p*	<0.001[d]	<0.001[e]	
Healthy side minus the patient's PPTs M (P25, P75), bf			
Erector spinae muscles			
Baseline	5.24 (3.50, 7.46)	4.86 (4.13, 6.48)	0.853[c]
1st treatment	3.31 (1.89, 5.25)	4.10 (3.11, 5.09)	0.099[c]
7st treatment	0.75 (0.19, 1.44)	2.20 (1.22, 3.49)	0.000[c]
10st treatment	0.47 (0.08, 1.25)	1.70 (1.01, 2.43)	0.000[c]
14st treatment	0.10 (−0.38, 0.58)	0.96 (0.55, 1.80)	0.000[c]
14st treatment-baseline	−4.92 (−7.00, −3.42)	−3.95 (−5.57, −2.30)	0.084[c]
p*	<0.001[d]	<0.001[e]	
Gluteus maximus muscles			
Baseline	5.82 (3.26, 7.46)	5.02 (3.38, 7.48)	0.702[c]
1st treatment	2.78 (1.74~ 3.82)	3.98 (3.13~ 4.82)	0.072[d]
7st treatment	0.32 (−0.46, 2.03)	2.53 (1.02, 4.00)	0.001[c]
10st treatment	0.65 (−0.35, 1.95)	1.64 (0.90, 339)	0.006[c]
14st treatment	0.71 (−0.32~ 0.46)	1.41 (0.87~ 1.95)	0.000[d]
14st treatment-baseline	−5.64 (−6.99~ −4.30)	−4.41 (−6.12~ −2.70)	0.257[d]
p*	<0.001[d]	<0.001[d]	
BDI-II M (P25, P75)			
Baseline	9.00 (4.00, 10.00)	9.00 (3.00, 13.50)	0.491[c]
14st treatment	2.00 (0.00, 5.00)	4.00 (0.00, 10.00)	0.049[d]
14st treatment-baseline	−5.00 (−7.00, −3.00)	−2.00 (−5.00, 0.00)	0.023[d]
p*	<0.001[d]	0.001[e]	
BAI M (P25, P75)			
Baseline	32.00 (27.00, 26.00)	30.00 (28.00, 36.00)	0.901[c]
14st treatment	27.00 (24.00, 28.00)	27.00 (26.00, 30.00)	0.364[d]
14st treatment-baseline	−3.00 (−8.00, −1.00)	−3.00 (−8.50, 0.00)	0.396[d]
p*	<0.001[e]	<0.001[e]	

Notes: [c]p-value from the Mann–Whitney *U*-test; [d]p-value from the paired-*t* test within-group; [e]p-value from the Wilcoxon test within-group.

Abbreviations: M, median; P25, 25th percentile; P75, 75th percentile; SF-MPQ, Simplified McGill Pain Questionnaire; PRI, Pain Rating Index; VAS, Visual Analog Scale; PPI, Present Pain Intensity; ODI, Oswestry Disability Index; PPT, Pain Pressure Threshold; BDI-II, Beck Depression Inventory-II; BAI, Beck Anxiety Inventory; p*, Comparison within the group before and after 14 days of treatment.

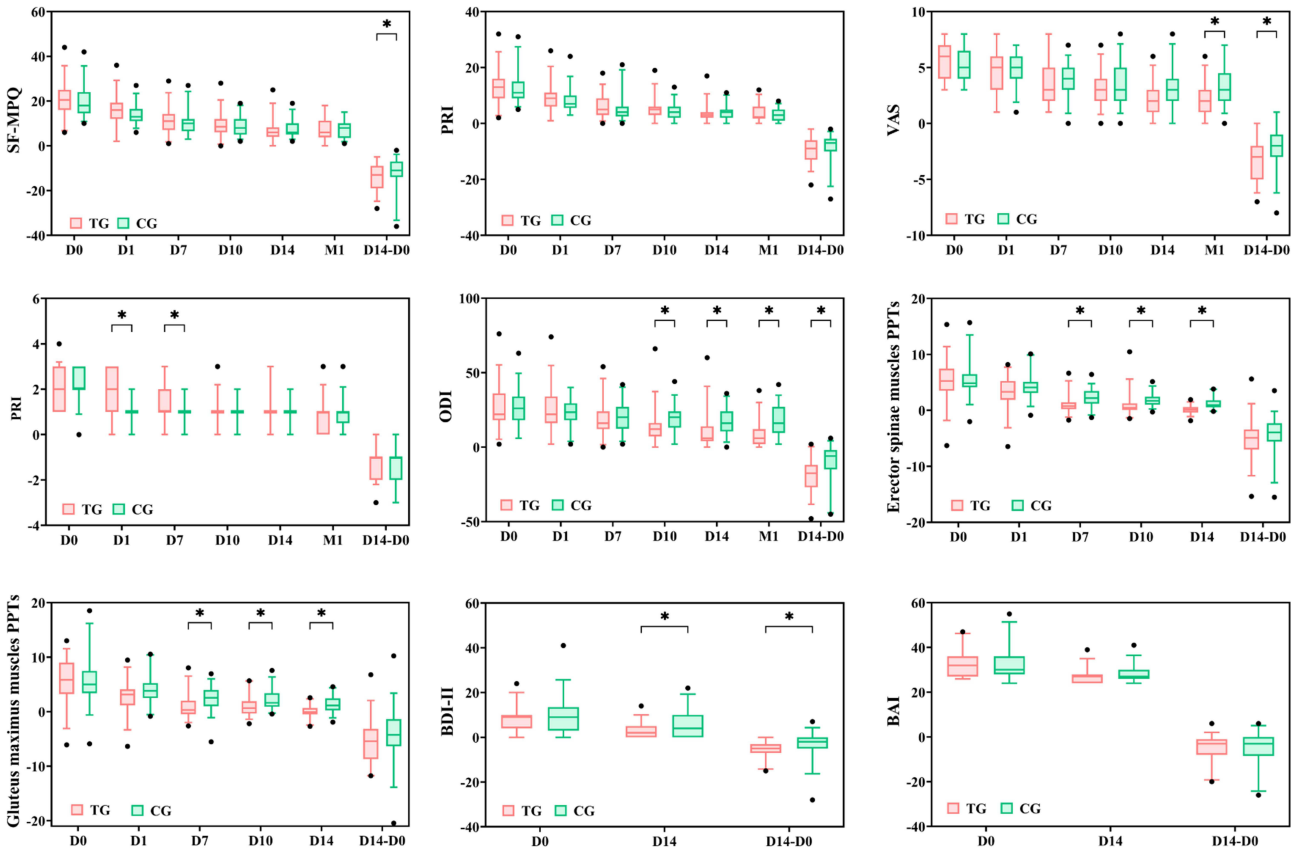

Figure 3 Comparison of clinical outcomes in the TG and CG subjects.*$P < 0.05$.
Abbreviations: SF-MPQ, Simplified McGill Pain Questionnaire; PRI, Pain Rating Index; VAS, Visual Analog Scale; PPI, Present Pain Intensity; ODI, Oswestry Disability Index; PPT, Pain Pressure Threshold; BDI-II, Beck Depression Inventory-II; BAI, Beck Anxiety Inventory; D0, day 0 of treatment; D1, day 1 of treatment; D7, day 7 of treatment; D10, day 10 of treatment; D14, day 14 of treatment; D14-D0, day 14 of treatment minus day 0 of treatment; M1, month 1 after treatment.

1-month post-treatment. We also evaluated changes in these indicators between baseline and day 14 of treatment for the two groups. Since the data for clinical outcomes was not normally distributed, it was presented using box plots and scatter plots.

Primary Outcome Measures

Compared to baseline, SF-MPQ scores on day 14 of treatment were significantly lower in both the TG patients [median = −13.00; (P25 = −19.00, P75 = −9.00); $P < 0.001$] and CG patients [−11.00 (−14.00, −7.00); $P < 0.001$]. Furthermore, SF-MPQ scores were significantly different between the TG and CG subjects on day 14 of treatment ($P < 0.05$) but were not significantly different at the 1-month follow-up ($P > 0.05$) (Table 2).

The VAS scores were significantly different between the TG and CG subjects on day 14 of treatment [TG: −3.00 (−5.00, −2.00); CG: −2.00 (−3.00, −1.00)] ($P < 0.05$). Furthermore, at the 1-month follow-up, VAS score of the TG subjects [2.00 (1.00, 3.00)] was significantly lower than the VAS score of the CG subjects [3.00 (2.00, 4.50)] ($P < 0.05$). Compared to the TG subjects, PPI scores were significantly lower in the CG subjects on treatment day 1 [1.00 (1.00, 2.00) vs 2.00 (1.00, 3.00); $P = 0.001$) and treatment day 7 [1.00 (1.00, 1.00) vs 1.00 (1.00, 2.00); $P = 0.001$].

Secondary Outcome Measures

Compared to baseline, PPT of the bilateral erector spinae [−4.92 (−7.00, −3.42); $P < 0.001$], PPT of the bilateral gluteus maximus [−5.64 (−6.99, −4.30); $P < 0.001$], ODI score [−17.60 (−27.00, −12.00); $P < 0.001$], BDI-II score [−5.00 (−7.00, −3.00); $P < 0.001$], and BAI score [−3.00 (−8.00, −1.00; $P < 0.001$] were significantly reduced in the TG subjects on treatment day 14. Furthermore, PPT of the bilateral erector spinae [−3.95 (−5.57, −2.30); $P < 0.001$], PPT of the bilateral gluteus maximus [−4.41 (−6.12, −2.70); $P < 0.001$], ODI score [−6.00 (−15.00, −2.00); $P < 0.001$], BDI-II score

https://doi.org/10.2147/JPR.S592723

[−2.00 (−5.00, 0.00); $P = 0.001$], and BAI score [−3.00 (−8.50, 0.00); $P < 0.001$] were also significantly reduced on treatment day 14 in the CG subjects compared to baseline.

The PPT of the TG subjects was significantly different than the CG subjects on days 7, 10, and 14 of treatment ($P < 0.05$). The ODI score of the TG subjects was also significantly different compared to the CG subjects on days 10 and 14 of treatment, as well as at the 1-month follow-up ($P < 0.05$). The BDI-II score was also significantly different between the TG and CG subjects on treatment day 14 ($P < 0.05$).

Brain Function Indicators

Abnormal Spontaneous Brain Activity in LDH Patients Before Intervention

The fALFF value was significantly lower in the left medial orbitofrontal cortex (mOFC.L) of LDH patients compared to the healthy controls. Furthermore, fALFF values were not significantly different between the TG and CG subjects (GRF-corrected voxel $P < 0.01$, cluster $P < 0.05$). Moreover, significant positive correlation was observed between the fALFF value in the brain region and pain duration in LDH patients (r = 0.251, $P = 0.035$). However, using the left medial orbitofrontal cortex as the seed point for FC analysis, significant differences were not detected between LDH patients and healthy controls in the FC between the mOFC.L and other brain regions.

Changes in Spontaneous Brain Activity After Tuina Intervention

The effects analysis of fMRI data demonstrated significant time × group interactions for fALFF in several brain regions, including right superior temporal gyrus pole (STG.pole.R), right middle frontal gyrus (MFG.R), inferior frontal gyrus, triangular part (IFGtri), left calcarine sulcus (CAL.L), and left thalamus (THA.L) (Figure 4). Furthermore, simple-effects analysis of fMRI data after 14 days of treatment showed that the fALFF values in the frontal regions such as IFGtri and MFG.R significantly decreased in the TG subjects ($P < 0.05$) but significantly increased in the CG subjects ($P < 0.05$). Moreover, fALFF values in the THA.L, CAL.L/Lingual, and STG.pole.R regions significantly increased in the TG subjects but significantly decreased in the CG subjects ($P < 0.05$) (Table 3).

The effects analysis of fMRI data for FC demonstrated significant time × group interactions of IFGtri.L with the left inferior parietal lobule (IPL.L), MFG.L, IFGtri.R, and Crus2.R, as well as IFGtri.R with IFGtri.L, right substantia nigra pars reticulata (SN_pr.R), and right cerebellar crus 1 (Crus1.R), and CAL.L with CAL.R (Figure 5). Furthermore, post-hoc multiple comparisons demonstrated that the FC of IFGtri.L with IPL.L, MFG.L, IFGtri.R, and right cerebellar crus 2 (Crus2.R), as well as FC of IFGtri.R with IFGtri.L, SN_pr.R, and Crus1.R were significantly reduced in the TG ($P < 0.05$), but significantly increased in the CG ($P < 0.05$). Moreover, FC of CAL.L with CAL.R was significantly increased in the TG subjects ($P < 0.05$) and significantly decreased in the CG subjects ($P < 0.05$) (Table 4).

Correlation Analysis Shows Clinical Improvement in the TG Subjects

Changes in the fALFF value of STG.pole.R positively correlated with improvements in ODI (r = 0.466, P = 0.011; Figure 6). Furthermore, changes in the fALFF value of IFGtri.L positively correlated with improvements in BAI (r = 0.500, $P = 0.006$), and changes in fALFF value of IFGtri.R positively correlated with improvements in BAI (r = 0.409, $P = 0.027$).

FC between IFGtri.R and SNpr.R showed a positive correlation with improvements in SF-MPQ scores (r = 0.511, $P = 0.005$). Furthermore, FC between IFGtri.L and IFGtri.R demonstrated a negative correlation with improvements in the PPT of gluteus maximus on the healthy side compared to the affected side (r = −0.518, $P = 0.004$). Moreover, FC between CAL.L and CAL.R showed a negative correlation with improvements in ODI (r = −0.418, $P = 0.024$) and BAI (r = −0.402, $P = 0.030$).

Among these correlations, the strongest associations were observed between increased functional connectivity of IFGtri.L with SNpr.R and reduction in SF-MPQ scores (r = 0.511, $P = 0.005$), and between decreased connectivity of IFGtri.L with IFGtri.R and improvement in pain pressure threshold (r = –0.518, $P = 0.004$).

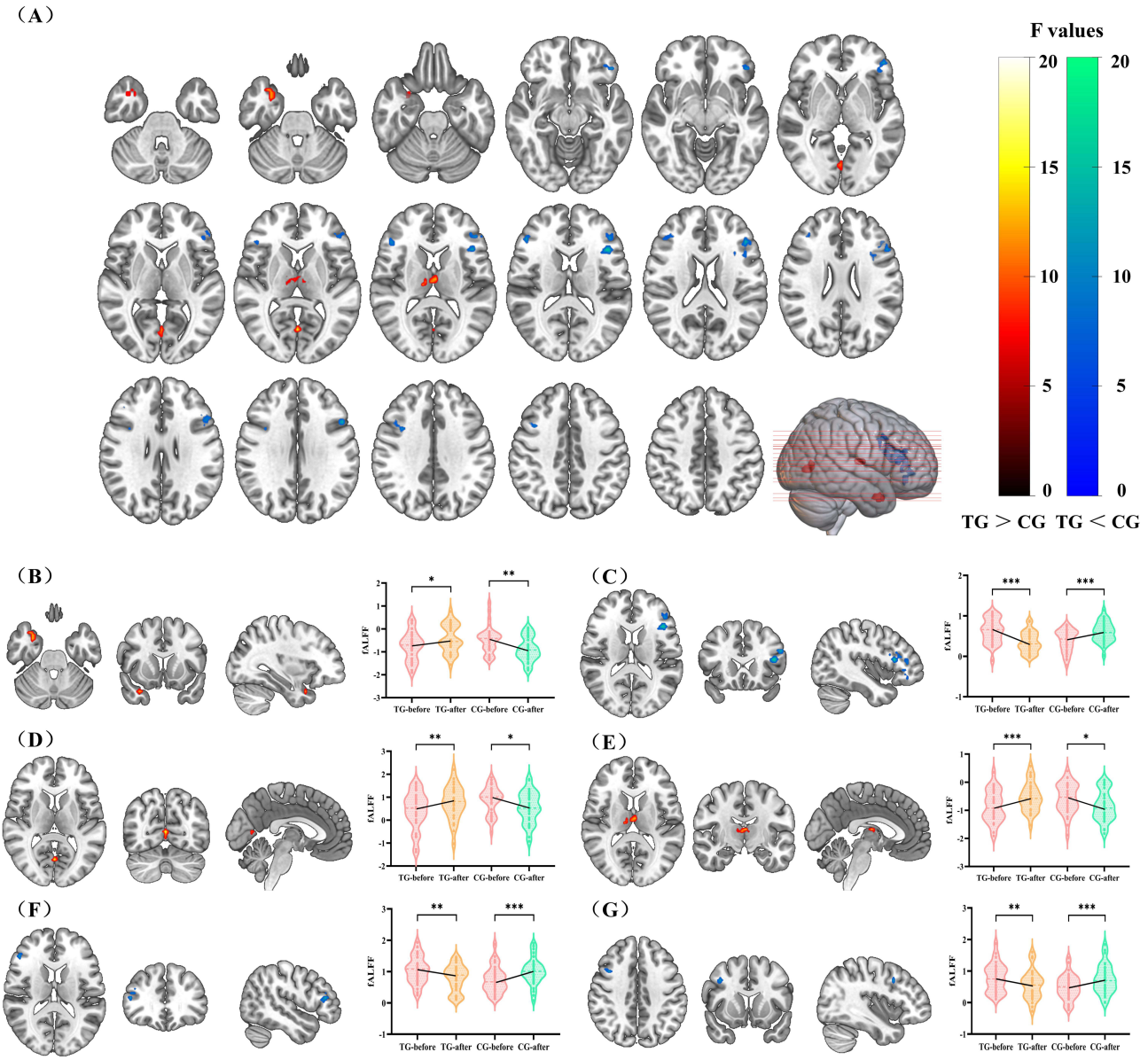

Figure 4 Brain regions with significant timexgroup interactions for fALFF in the CG and TG subjects before and after treatment.
Notes: (**A**) Brain regions in which fALFF shows significant timexgroup interaction. (**B**) Changes and Trends of STG.bole.R in fALFF Values. (**C**) Changes and Trends of IFGtri. L in fALFF Values. (**D**) Changes and Trends of CAL.L in fALFF Values; (**E**) Changes and Trends of THA.L in fALFF Values. (**F**) Changes and Trends of IFGtri.R in fALFF Values. (**G**) Changes and Trends of MFG.R in fALFF Values. *$P < 0.05$; **$P < 0.01$; ***$P < 0.001$.
Abbreviations: STG.pole, superior temporal gyrus pole; IFGtri, inferior frontal gyrus, triangular part; CAL, calcarine sulcus; THA, thalamus; MFG, middle frontal gyrus; TG, test group; CG, control group.

Medication Use

During the treatment period, neither group of patients used painkillers for lumbar or leg pain. However, in the TG, one patient took 0.3g of sustained-release ibuprofen capsules twice daily for 2 days due to fever and discontinued the medication once the body temperature returned to normal.

Safety Evaluation

We also evaluated the safety of Tuina in 72 LDH patients. Three TG subjects without previous history of Tuina experienced mild tenderness at the treatment site after the first session. However, significant adverse events were not reported in the CG subjects. The mild tenderness in the TG subjects was resolved within 3 days of follow-up.

https://doi.org/10.2147/JPR.S592723

https://doi.org/10.2147/JPR.S592723

Table 3 ANCOVA Evaluation of Neuroimaging Outcomes in fALFF with Time and Group as Factors

Brain Area	Cluster Size	Peak Value	Peak Coordinate in MNI Space			Time	Test Group (n=29)	Control Group (n=33)	p-value
			x	y	z				
STG.pole.R	26	14.56	33	12	−30	Baseline (mean ± SD)	−0.75 ± 0.12	−0.48 ± 0.10	p^{T}=0.578
						14st treatment-baseline (difference, 95% CI)	0.32 (0.08 to 0.56)	–0.41 (−0.67 to −0.16)	p^{T*G}=0.0001
									p^{G}=0.002
IFGtri.L	121	17.87	−42	21	15	Baseline (mean ± SD)	0.62 ± 0.30	0.37 ± 0.27	p^{T}=0.282
						14st treatment-baseline (difference, 95% CI)	–0.28 (−0.37 to −0.18)	0.21(−0.12 to −0.30)	p^{T*G}<0.0001
									p^{G}=0.0002
CAL.L	25	18.03	0	−69	9	Baseline (mean ± SD)	0.43 ± 0.27	0.88 ± 0.80	p^{T}=0.988
						14st treatment-baseline (difference, 95% CI)	0.32(0.11 to 0.54)	0.32 (0.56 to 0.81)	p^{T*G}=0.0001
									p^{G}=0.254
THA.L	26	15.20	−3	−12	12	Baseline (mean ± SD)	0.86 ± 0.57	0.57 ± 0.53	p^{T}=0.791
						14st treatment-baseline (difference, 95% CI)	0.32 (0.17 to 0.46)	0.28 (0.50 to 0.07)	p^{T*G}<0.0001
									p^{G}=0.002
IFGtri.R	26	15.24	48	33	15	Baseline (mean ± SD)	1.05 ± 0.43	0.74 ± 0.42	p^{T}=0.978
						14st treatment-baseline (difference, 95% CI)	–0.26(−4.2 to −0.94)	0.26 (0.13 to 0.39)	p^{T*G}<0.0001
									p^{G}=0.0004
MFG.R	18	15.31	39	12	39	Baseline (mean ± SD)	0.79 ± 0.45	0.49 ± 0.39	p^{T}=0.785
						14st treatment-baseline (difference, 95% CI)	–0.23 (−0.36 to −0.10)	0.26 (0.12 to 0.39)	p^{T*G}<0.0001
									p^{G}=0.0001

Notes: T indicates p-values between different time points; T*G indicates p-values for Time*Group interactions. G indicates p-values between different groups.

Abbreviations: STG.pole, superior temporal gyrus pole; IFGtri, inferior frontal gyrus, triangular part; CAL, calcarine sulcus; THA, thalamus; MFG, middle frontal gyrus; SD, standard deviation; L, the left hemisphere; R, the right hemisphere.

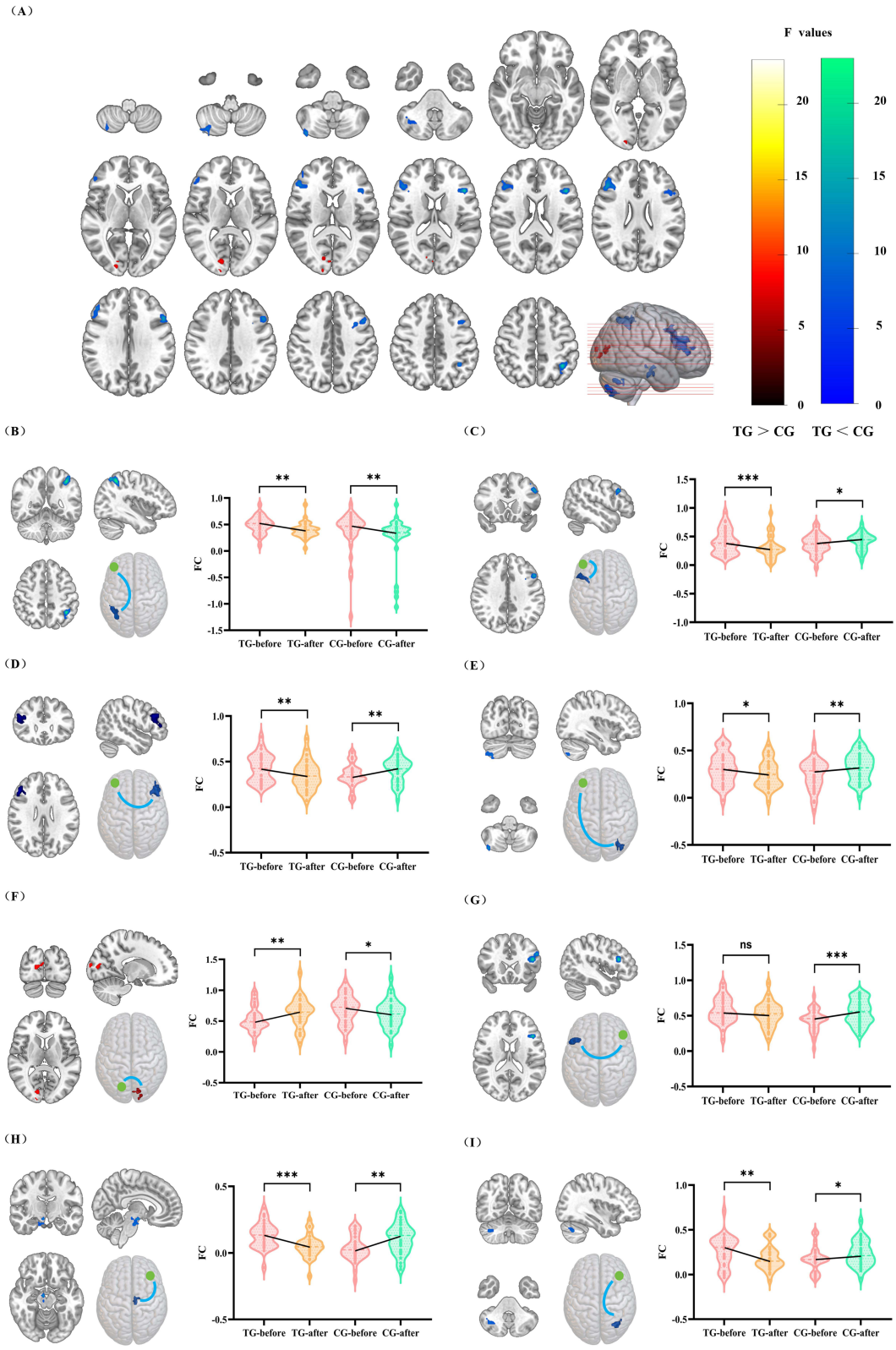

Figure 5 Brain regions with significant time×group interactions for FC in the CG and TG subjects before and after treatment.
Notes: (**A**) Brain regions in which FC shows significant time × group interaction. (**B**) Changes and Trends of IFGtri.L–IPL.L in FC Values. (**C**) Changes and Trends of IFGtri.L–MFG.L in FC Values.; (**D**) Changes and Trends of IFGtri.L–IFGtri.R in FC Values. (**E**) Changes and Trends of IFGtri.L–Cere_Crus2.R in FC Values. (F). Changes and Trends of CAL.L–CAL.R in FC Values. (**G**) Changes and Trends of IFGtri.R–IFGtri.L in FC Values. (**H**) Changes and Trends of IFGtri.R–SN_pr.R in FC Values. (**I**) Changes and Trends of IFGtri.R–Cere_Crus1.R in FC Values. *$P < 0.05$; **$P < 0.01$; ***$P < 0.001$.
Abbreviations: IFGtri, inferior frontal gyrus, triangular part; IPL, inferior parietal lobule; MFG, middle frontal gyrus; Cere_Crus2, cerebellar crus 2; CAL, calcarine sulcus; SN_pr, substantia nigra pars reticulata; Cere_Crus1, cerebellar crus 1; TG, test group; CG, control group; ns, not significant.

https://doi.org/10.2147/JPR.S592723

https://doi.org/10.2147/JPR.S592723

Table 4 ANCOVA Evaluation of Neuroimaging Outcomes in FC with Time and Group as Factors

Seed Region	Peak Location of the Cluster	Cluster size	Peak Value	Peak Coordinate in MNI Space			Time	Test Group (n=29)	Control Group (n=33)	p-value
				x	y	z				
IFGtri.L	IPL.L	88	21.61	−39	−51	51	Baseline (mean±SD)	0.49 ± 0.16	0.37 ± 0.16	p^{T}=0.467
							14st treatment-baseline (difference, 95% CI)	– 0.08 (−0.12 to −0.04)	0.06(0.02 to 0.10)	p^{T*G}<0.0001 p^{G}=0.320
	MFG.L	66	15.33	−51	18	36	Baseline (mean±SD)	0.41 ± 0.21	0.36 ± 0.17	p^{T}=0.176
							14st treatment-baseline (difference, 95% CI)	– 0.10 (−0.14 to −0.05)	–0.05 (0.01 to 0.10)	p^{T*G}=0.00002 p^{G}=0.032
	IFGtri.R	133	15.21	48	27	27	Baseline (mean±SD)	0.43 ± 0.15	0.35 ± 0.13	p^{T}=0.452
							14st treatment-baseline (difference, 95% CI)	– 0.08 (−0.12 to −0.04)	0.06 (0.02 to 0.10)	p^{T*G}<0.0001 p^{G}=0.124
	Cere_Crus2.R	43	14.14	39	−81	−45	Baseline (mean±SD)	0.31 ± 0.16	0.24 ± 0.16	p^{T}=0.473
							14st treatment-baseline (difference, 95% CI)	−0.06 (−0.10 to −0.01)	0.08 (0.04 to 0.12)	p^{T*G}=0.0005 p^{G}=0.0005
CAL.L	CAL.R	41	9.53	15	−84	9	Baseline (mean±SD)	0.53 ± 0.20	0.70 ± 0.22	p^{T}=0.533
							14st treatment-baseline (difference, 95% CI)	0.11 (0.04 to 0.19)	–0.08 (−0.16 to −0.01)	p^{T*G}<0.0001 p^{G}=0.036
IFGtri.R	IFGtri.L	65	19.68	−45	21	18	Baseline (mean±SD)	0.57 ± 0.10	0.44 ± 0.09	p^{T}=0.109
							14st treatment-baseline (difference, 95% CI)	–0.05 (−0.10 to 0.00)	0.11 (0.06 to0.16)	p^{T*G}<0.0001 p^{G}=0.00004
	SN_pr.R	34	16.15	6	−12	−15	Baseline (mean±SD)	0.13 ± 0.18	0.03 ± 0.14	p^{T}=0.744
							14st treatment-baseline (difference, 95% CI)	– 0.08 (−0.12 to −0.04)	0.07 (0.02 to0.12)	p^{T*G}<0.0001 p^{G}=0.001
	Cere_Crus1.R	38	11.31	36	−63	−39	Baseline (mean±SD)	0.27 ± 0.17	0.18 ± 0.14	p^{T}=0.450
							14st treatment-baseline (difference, 95% CI)	– 0.08 (−0.14 to −0.03)	0.06 (0.01 to0.11)	p^{T*G}<0.0001 p^{G}=0.175

Notes: T indicates p-values between different time points; T*G indicates p-values for Time*Group interactions. G indicates p-values between different groups.

Abbreviations: IFGtri, inferior frontal gyrus, triangular part; IPL, inferior parietal lobule; MFG, middle frontal gyrus; Cere_Crus2, cerebellar crus 2; CAL, calcarine sulcus; SN_pr, substantia nigra pars reticulata; Cere_Crus1, cerebellar crus 1; SD, standard deviation.

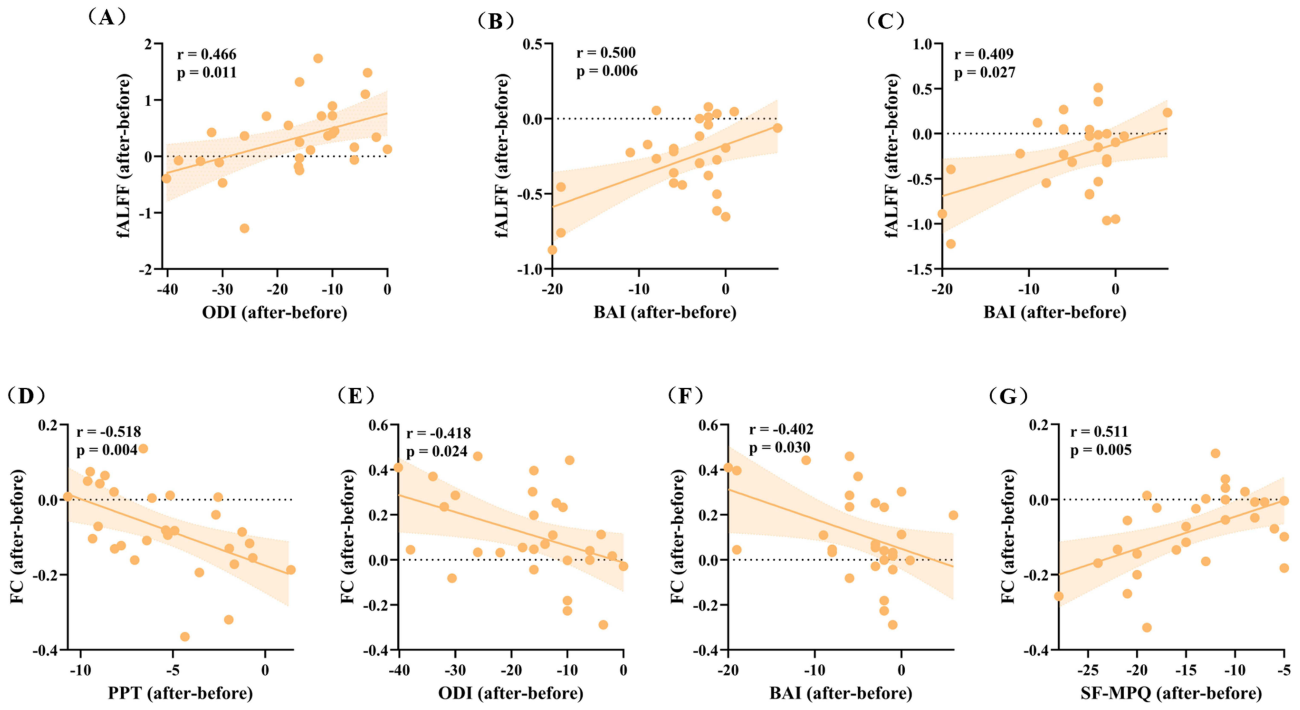

Figure 6 Correlations between fALFF and FC of various brain regions with clinical improvements in TG after treatments.
Notes: (**A**) STG.bole.R (**B**) IFGtri.L (**C**) IFGtri.R (**D**) IFGtri.L–IFGtri.R (**E**) CAL.L–CAL.R (**F**) CAL.L–CAL.R (**G**) IFGtri.R–SN_pr.R.
Abbreviations: IFGtri, inferior frontal gyrus, triangular part; CAL, calcarine sulcus; SN_pr, substantia nigra pars reticulata; ODI, Oswestry Disability Index; BAI, Beck Anxiety Inventory; PPT, Pain Pressure Threshold; SF-MPQ, Simplified McGill Pain Questionnaire.

Discussion

In this study, we conducted as a randomized controlled neuroimaging trial and demonstrated that Tuina was more effective in treating LDH patients than TENS combined with lumbar traction and improved their pain symptoms, lumbar function, and depressive symptoms. This is the first study to identify the central mechanisms underlying the analgesic effects of Tuina from the perspective of multi-regional brain functional reorganization and neural network interactions. Therefore, results of this study offer neuroimaging evidence supporting the underlying mechanism of Tuina therapy.

Clinically, the TG subjects showed significantly higher improvements in SF-MPQ, VAS, PPT, ODI, and BDI-II scores compared to the CG. This was in alignment with previous findings[34,35] and suggested that Tuina regulates muscle tension and improves circulation via mechanical stimulation. This multi-target mechanism offers unique benefits for managing chronic pain. Although TENS combined with traction therapy showed an immediate effect on pain relief after the first intervention, as shown by lower PPI scores, no significant difference in PPI was observed between the two groups after 14 days of treatment. This suggests that TENS combined with traction therapy may be more suitable for the acute LDH pain but its long-term effects are limited.[36,37] In contrast, the analgesic effects of Tuina therapy are more pronounced over time. This suggests that Tuina was associated with central sensitization and pain memory formation. These brain-related mechanisms were further investigated by neuroimaging.

Neuroimaging studies[38,39] suggest that patients with chronic pain have significantly higher activity in the IFGtri and MFG, and reduced activity in the STG.pole, IPL, THA, and CAL. IFGtri is a core component of the ventral attention network (VAN), which responds rapidly to sudden changes in environmental cues and reorients attention accordingly.[40] STG.pole is an essential component of the auditory network (AUN) and plays a key role in the regulation of pain perception.[41] Both MFG and IPL are critical regions in the default mode network (DMN) of the brain and are essential for processing pain memory.[42] THA plays a key role in pain processing and the reward system, thereby modulating pain perception.[43] CAL is an essential component of the visual network (VIN) and is involved in the suppression of somatic pain signals and allocation of attention.[44] Together, these findings indicate that chronic pain patients exhibit disruptions in

https://doi.org/10.2147/JPR.S592723

multiple networks such as VAN, AUN, DMN, and VIN, resulting in impaired pain perception, emotional processing, cognitive integration, and reward regulation.

This study showed that Tuina exerts analgesic effects by inhibiting the IFGtri and enhancing spontaneous neural activity in the STG.pole.R, THA.L, and CAL.L. Abnormal activity in the IFGtri suggests increased sensitivity to pain stimuli in the LDH patients. Tuina potentially alleviates pain by reducing the patients' focus on pain by suppressing the functional state of the IFGtri. Functional activity of the STG.pole.R is significantly associated with the quality of life in LDH patients.[45] Chronic pain induces aversion and fear, leading to reduced functional activity in the STG.pole.R. This study confirmed that Tuina intervention effectively increases the ALFF value of the STG.pole.R. This suggests that Tuina improves pain perception by modulating the negative perception of pain in LDH patients.[46] Thalamus is the primary brain region for activity modulation in chronic pain patients.[47] Our results also confirmed that Tuina enhances THA function by reducing the alertness levels and strengthening reward feedback, thereby alleviating pain-related distress in LDH patients. Furthermore, LDH patients exhibit enhanced functional connectivity in the DMN.[48] CAL/Lingual, a key node linking the VIN and DMN, leverages visual cues to effectively shift attention and increase pain thresholds.[49] This method has been consistently validated in clinical studies.[50,51]

Our data also showed that Tuina decreased the functional connectivity of IFGtri.L with IFGtri.R, MFG.L, IPL.L, and Crus2.R Previous studies[40] have shown that IFGtri.L inhibits transmission of signals that are not related with pain, whereas IFGtri.R suppresses premature pain signals. Therefore, decreased functional connectivity between IFGtri.L and IFGtri.R suggests that Tuina enhances pain tolerance by modulating the transmission of pain signals. Furthermore, the analgesic effect of Tuina involves MFG.R and IPL.L, which not only predict changes in pain perception after Tuina but also undergo functional reorganization.[21,52] Therefore, decreased functional connectivity of IFGtri.L with IPL.L and MFG.L indicates that Tuina enhances pain cognition by inhibiting amplification of pain signals. Moreover, Tuina inhibits the functional connectivity of IFGtri.R with Crus1.R and SN_pr.R. Crus1.R and Crus2.R play a key role in regulating sensitivity to noxious pain stimuli.[53] Our study showed decreased functional connectivity of IFGtri.R with Crus1.R and Crus2.R, thereby suggesting that Tuina therapy effectively suppresses pain sensitivity in LDH patients. Neurons in SN_pr.R facilitate the maintenance of pain by regulating dopamine activity.[54] The reduced functional connectivity between IFGtri.R and SN_pr.R suggests that Tuina inhibits dopamine activity, thereby interrupting the chronic progression of pain. We also observed that Tuina enhanced the functional connectivity between CAL.L and CAL.R. This indicates that Tuina reduces somatic pain signals by coordinating attention distribution across both sides. These results indicate that Tuina modulates pain perception, emotional regulation, attentional shifts, and reward processes in LDH patients through brain function reorganization and synergistic effects of executive control, auditory, default, and visual networks.

Further correlational analysis suggested that the modulation of specific brain regions by Tuina was significantly associated with the improvement of clinical symptoms in LDH. Changes in the functional connectivity strength between IFGtri.R and SN_pr.R were significantly associated with improvements in the SF-MPQ scores, thereby suggesting that this pathway mediated the analgesic effect through the dopaminergic reward system.[54] Furthermore, modulation of the functional connectivity between IFGtri.L and IFGtri.R by Tuina was significantly correlated with improvements in PPT and BAI. This suggested that Tuina may enhance pain signal transmission in the bilateral inferior frontal gyrus, thereby increasing the threshold for somatic pain and alleviating the anxiety associated with LDH pain. Moreover, changes in the STG.pole.R functional area by Tuina were significantly associated with improvements in ODI, whereas changes in functional connectivity between CAL.L and CAL.R were significantly associated with improvements in both BAI and ODI. These findings suggested that improvement in the lumbar function of LDH patients by Tuina intervention was closely linked with inhibition of pain signal transmission, thereby restoring the normal perception of pain. These findings highlight that modulation of the inferior frontal triangularis, particularly its connectivity with subcortical reward-related regions and the contralateral homotopic area, may represent a core neural mechanism underlying Tuina's analgesic and somatosensory effects. The IFGtri is a key node of the ventral attention network, and its altered connectivity with the SNpr—a region involved in dopamine-mediated pain modulation—suggests that Tuina may engage both attentional and reward circuits to alleviate pain.

This study has a few limitations. A double-blind design could not be implemented because of the unique nature of Tuina therapy. This may have led to potential bias because subjective judgments, attentional or expectancy effects of patients may

have influenced the evaluation results. However, the study rigorously followed standardized procedures and uniform evaluation criteria to minimize potential bias in the results. In addition, the 14 days intervention period limits the conclusion on long-term neural reorganization and the persistence of effects. To further enhance the reliability of findings, future studies should include multi-center, long-term follow-up clinical trials and engage third-party evaluation teams to establish a more objective efficacy assessment system and ensure generalizability of the results. Furthermore, we plan to perform subgroup analyses of patients with LDH by integrating functional neuroimaging techniques to systematically investigate the dose–response relationship between pain types, herniated disc features, and activation patterns in specific brain regions. This will provide a robust, evidence-based foundation for developing precise rehabilitation plans.

Conclusion

In summary, treatment efficacy of Tuina was superior than TENS combined with lumbar traction therapy in LDH patients. Tuina significantly reduced pain and improved brain function in specific regions related with pain and negative emotions. LDH patients exhibit functional abnormalities across multiple networks, including VAN, AUN, DMN, and VIN. The IFGtri plays a key role in mediating the efficacy of Tuina therapy for LDH. From a rehabilitation perspective, these results provide preliminary evidence that Tuina may be prioritized as an effective non-pharmacological intervention for LDH. Meanwhile, this also suggests that targeting brain functional plasticity, especially in the IFGtri, may provide a basis for neural regulation therapy strategies for chronic pain.

Data Sharing Statement

The datasets are available from the corresponding author on reasonable request.

Ethics Approval and Informed Consent

This study complies with the Declaration of Helsinki and has been approved by the Ethics Review Committee of the Rehabilitation Hospital Affiliated of Fujian University of Traditional Chinese Medicine (Ethical Approval No: 2024KY-008-02), and was registered with the Chinese Clinical Trial Registry (Registration No: ChiCTR2400083784). All the enrolled subjects were required to provide written informed consent.

Consent for Publication

The details of any images, videos, recordings, etc. can be published, and that the person(s) providing consent has been shown the article contents to be published.

Acknowledgments

Acknowledgments are due to all study participants.

Author Contributions

All authors made a significant contribution to the work reported, whether that is in the conception, study design, execution, acquisition of data, analysis, and interpretation, or in all these areas; took part in drafting, revising, or critically reviewing the article; gave final approval of the version to be published; have agreed on the journal to which the article has been submitted; and agree to be accountable for all aspects of the work.

Funding

This work was supported by the National Natural Science Foundation of China (grant no. 82575244, 82105039), the Key Research Project of Chinese Association of Rehabilitation Medicine (grant no. KFKT-2024-KY-005), the Fujian Research and Training Grants for Young and Middle-aged Leaders in Healthcare, the Project of Natural Science Foundation of Fujian Province (grant no. 2023J06037), Management Project of Fujian University of Traditional Chinese Medicine (grant no. XB2024062), Fujian Provincial Marxism-Guided Fundamental Research Project in Philosophy and Social Sciences (grant no. FJ2025MGCA039).

Disclosure

The authors report no conflicts of interest in this work.

References

1. Yu P, Mao F, Chen J, et al. Characteristics and mechanisms of resorption in lumbar disc herniation. *Arthritis Res Ther*. 2022;24(1):205. doi:10.1186/s13075-022-02894-8
2. Zhang AS, Xu A, Ansari K, et al. Lumbar disc herniation: diagnosis and management. *Am J Med*. 2023;136(7):645–651. doi:10.1016/j.amjmed.2023.03.024
3. Cheng M, Xue Y, Cui M, et al. Global, regional, and national burden of low back pain: findings from the global burden of disease study 2021 and projections to 2050. *Spine*. 2025;50(7):E128–E139. doi:10.1097/BRS.0000000000005265
4. Dieleman JL, Cao J, Chapin A, et al. US health care spending by payer and health condition, 1996-2016. *JAMA*. 2020;323(9):863–884. doi:10.1001/jama.2020.0734
5. Andersson GB. Epidemiological features of chronic low-back pain. *Lancet*. 1999;354(9178):581–585. doi:10.1016/S0140-6736(99)01312-4
6. Peng B, Fu X, Pang X, et al. Prospective clinical study on natural history of discogenic low back pain at 4 years of follow-up. *Pain Physician*. 2012;15(6):525–532.
7. Furlan AD, Sandoval JA, Mailis-Gagnon A, Tunks E. Opioids for chronic noncancer pain: a meta-analysis of effectiveness and side effects. *CMAJ Can Med Assoc J*. 2006;174(11):1589–1594. doi:10.1503/cmaj.051528
8. Martell BA, O'Connor PG, Kerns RD, et al. Systematic review: opioid treatment for chronic back pain: prevalence, efficacy, and association with addiction. *Ann Intern Med*. 2007;146(2):116–127. doi:10.7326/0003-4819-146-2-200701160-00006
9. Pocratsky AM, Nascimento F, Özyurt MG, et al. Pathophysiology of Dyt1-Tor1a dystonia in mice is mediated by spinal neural circuit dysfunction. *Sci Transl Med*. 2023;15(694):eadg3904. doi:10.1126/scitranslmed.adg3904
10. Wang K, Cai B, Song Y, Chen Y, Zhang X. Somatosensory neuron types and their neural networks as revealed via single-cell transcriptomics. *Trends Neurosci*. 2023;46(8):654–666. doi:10.1016/j.tins.2023.05.005
11. Fuller AM, Luiz A, Tian N, et al. Gate control of sensory neurotransmission in peripheral ganglia by proprioceptive sensory neurons. *Brain*. 2023;146(10):4033–4039. doi:10.1093/brain/awad182
12. Huang S, Wakaizumi K, Wu B, et al. Whole-brain functional network disruption in chronic pain with disk herniation. *Pain*. 2019;160(12):2829–2840. doi:10.1097/j.pain.0000000000001674
13. Shen W, Tu Y, Gollub RL, et al. Visual network alterations in brain functional connectivity in chronic low back pain: a resting state functional connectivity and machine learning study. *Neuroimage Clin*. 2019;22:101775. doi:10.1016/j.nicl.2019.101775
14. Cheng ZJ, Zhang SP, Gu YJ, et al. Effectiveness of Tuina therapy combined with Yijinjing exercise in the treatment of nonspecific chronic neck pain: a randomized clinical trial. *JAMA Network Open*. 2022;5(12):e2246538. doi:10.1001/jamanetworkopen.2022.46538
15. Xu H, Zhao C, Guo G, et al. The effectiveness of Tuina in relieving pain, negative emotions, and disability in knee osteoarthritis: a randomized controlled trial. *Pain Med*. 2023;24(3):244–257. doi:10.1093/pm/pnac127
16. Mak S, Allen J, Begashaw M, et al. Use of massage therapy for pain, 2018-2023. *JAMA Network Open*. 2024;7(7):e2422259. doi:10.1001/jamanetworkopen.2024.22259
17. Wu Z, Guo G, Zhang Y, et al. Resting-state functional magnetic resonance imaging reveals brain remodeling after Tuina therapy in neuropathic pain model. *Front Mol Neurosci*. 2023;16:1231374. doi:10.3389/fnmol.2023.1231374
18. Kwon D. Brain imaging: FMRI advances make scans sharper and faster. *Nature*. 2023;617(7961):640–642. doi:10.1038/d41586-023-01616-7
19. Song S, Fang Y, Wan X, et al. Changes of regional brain activity following Tuina therapy for patients with painful cervical spondylosis: a resting-state fMRI study. *Front Neurol*. 2024;15:1399487. doi:10.3389/fneur.2024.1399487
20. Zhou XC, Wu S, Wang KZ, et al. Default mode network and dorsal attentional network connectivity changes as neural markers of spinal manipulative therapy in lumbar disc herniation. *Sci Rep*. 2024;14(1):29541. doi:10.1038/s41598-024-81126-2
21. Chen XM, Wen Y, Chen S, et al. Traditional Chinese Manual Therapy (Tuina) reshape the function of default mode network in patients with lumbar disc herniation. *Front Neurosci*. 2023;17:1125677. doi:10.3389/fnins.2023.1125677
22. Desmond JE, Glover GH. Estimating sample size in functional MRI (fMRI) neuroimaging studies: statistical power analyses. *J Neurosci Methods*. 2002;118(2):115–128. doi:10.1016/s0165-0270(02)00121-8
23. Jiang C, Huang H, Chen L, et al. Functional magnetic resonance imaging analysis of the clinical effect and cerebral mechanism of Tuina in lumbar disc herniation: protocol for a randomized controlled parallel group trial. *JMIR Res Protoc*. 2024;13(e63852). doi:10.2196/63852
24. Kreiner DS, Hwang SW, Easa JE, et al. An evidence-based clinical guideline for the diagnosis and treatment of lumbar disc herniation with radiculopathy. *Spine J*. 2014;14(1):180–191. doi:10.1016/j.spinee.2013.08.003
25. Fan B. *Massage Therapy*. China Traditional Chinese Medicine Press; 2016.
26. Zhou YF. *Massage Techniques*. China Traditional Chinese Medicine Press; 2021.
27. Hawker GA, Mian S, Kendzerska T, French M. Measures of adult pain: visual analog scale for pain (VAS pain), numeric rating scale for pain (NRS pain), McGill pain questionnaire (MPQ), short-form McGill pain questionnaire (SF-MPQ), chronic pain grade scale (CPGS), short form-36 bodily pain scale (SF-36 BPS), and measure of intermittent and constant osteoarthritis pain (ICOAP). *Arthritis Care Res*. 2011;63(11):S240–252. doi:10.1002/acr.20543
28. Fairbank JC, Pynsent PB. The oswestry disability index. *Spine*. 2000;25(22):2940–2952. doi:10.1097/00007632-200011150-00017.
29. Beck AT, Steer RA. *Manual for the Beck Depression Inventory*. Psychological Corporation; 1996.
30. Beck AT, Epstein N, Brown G, Steer RA. An inventory for measuring clinical anxiety: psychometric properties. *J Consult Clin Psychol*. 1988;56(6):893–897. doi:10.1037//0022-006x.56.6.893
31. Jenkinson M, Bannister P, Brady M, Smith S. Improved optimization for the robust and accurate linear registration and motion correction of brain images. *Neuroimage*. 2002;17(2):825–841. doi:10.1016/s1053-8119(02)91132-8
32. Candemir C. Spatial smoothing effect on group-level functional connectivity during resting and task-based fMRI. *Sens*. 2023;23(13):5866. doi:10.3390/s23135866

33. Caballero-Gaudes C, Reynolds RC. Methods for cleaning the BOLD fMRI signal. *Neuroimage*. 2017;154:128–149. doi:10.1016/j.neuroimage.2016.12.018
34. Zhang K, Ding L, Wang X, et al. Evidence of mirror therapy for recruitment of ipsilateral motor pathways in stroke recovery: a resting fMRI study. *Neurotherapeutics*. 2024;21(2):e00320. doi:10.1016/j.neurot.2024.e00320
35. Johnson MI, Paley CA, Jones G, Mulvey MR, Wittkopf PG. Efficacy and safety of transcutaneous electrical nerve stimulation (TENS) for acute and chronic pain in adults: a systematic review and meta-analysis of 381 studies (the meta-TENS study). *BMJ Open*. 2022;12(2):e051073. doi:10.1136/bmjopen-2021-051073
36. Qin X, Sun K, Xu W, et al. An evidence-based guideline on treating lumbar disc herniation with traditional Chinese medicine. *J Evid Based Med*. 2024;17(1):187–206. doi:10.1111/jebm.12598
37. Knotkova H, Hamani C, Sivanesan E, et al. Neuromodulation for chronic pain. *Lancet*. 2021;397(10289):2111–2124. doi:10.1016/S0140-6736(21)00794-7
38. Wang W, Long F, Wu X, Li S, Lin J. Clinical efficacy of mechanical traction as physical therapy for lumbar disc herniation: a meta-analysis. *Comput Math Methods Med*. 2022;2022:5670303. doi:10.1155/2022/5670303
39. Chen X, Chen N, Lai P, et al. Multimodal abnormalities of brain function in chronic low back pain: a systematic review and meta-analysis of neuroimaging studies. *Front Neurosci*. 2025;19:1535288. doi:10.3389/fnins.2025.1535288
40. Maulitz L, Nehls S, Stickeler E, et al. Psychological characteristics and structural brain changes in women with endometriosis and endometriosis-independent chronic pelvic pain. *Hum Reprod*. 2024;39(11):2473–2484. doi:10.1093/humrep/deae207
41. Corbetta M, Shulman GL. Control of goal-directed and stimulus-driven attention in the brain. *Nat Rev Neurosci*. 2002;3(3):201–215. doi:10.1038/nrn755
42. Harte SE, Wiseman J, Wang Y, et al. Experimental pain and auditory sensitivity in overactive bladder syndrome: a symptoms of the lower urinary tract dysfunction research network (LURN) study. *J Urol*. 2022;207(1):161–171. doi:10.1097/JU.0000000000002147
43. Antoniou G, Lambourg E, Steele JD, Colvin LA. The effect of adverse childhood experiences on chronic pain and major depression in adulthood: a systematic review and meta-analysis. *Br J Anaesth*. 2023;130(6):729–746. doi:10.1016/j.bja.2023.03.008
44. Satterthwaite TD, Kable JW, Vandekar L, et al. Common and dissociable dysfunction of the reward system in bipolar and unipolar depression. *Neuropsychopharmacol*. 2015;40(9):2258–2268. doi:10.1038/npp.2015.75
45. Diano M, D'Agata F, Cauda F, et al. Cerebellar clustering and functional connectivity during pain processing. *Cerebellum*. 2016;15(3):343–356. doi:10.1007/s12311-015-0706-4
46. Ge X, Wang L, Pan L, et al. Alteration of the cortical morphology in classical trigeminal neuralgia: voxel-, deformation-, and surface-based analysis. *J Headache Pain*. 2023;24(1):17. doi:10.1186/s10194-023-01544-x
47. Zhou XC, Wu S, Wang KZ, et al. Impact of spinal manipulative therapy on brain function and pain alleviation in lumbar disc herniation: a resting-state fMRI study. *Chin J Integr Med*. 2025;31(2):108–117. doi:10.1007/s11655-024-4205-7
48. Nüssel M, Zhao Y, Knorr C, et al. Deep brain stimulation, stereotactic radiosurgery and high-intensity focused ultrasound targeting the limbic pain matrix: a comprehensive review. *Pain Ther*. 2022;11(2):459–476. doi:10.1007/s40122-022-00381-1
49. Pei Y, Zhang Y, Zhu Y, et al. Hyperconnectivity and high temporal variability of the primary somatosensory cortex in low-back-related leg pain: an fMRI study of static and dynamic functional connectivity. *J Pain Res*. 2020;13:1665–1675. doi:10.2147/JPR.S242807
50. Jauniaux J, Khatibi A, Rainville P, Jackson PL. A meta-analysis of neuroimaging studies on pain empathy: investigating the role of visual information and observers' perspective. *Soc Cogn Affect Neurosci*. 2019;14(8):789–813. doi:10.1093/scan/nsz055
51. Carwile JL, Feldman S, Johnson NR. Use of a simple visual distraction to reduce pain and anxiety in patients undergoing colposcopy. *J Low Genit Tract Dis*. 2014;18(4):317–321. doi:10.1097/LGT.0000000000000024
52. Xiaolian J, Xiaolin L, Lan ZH. Effects of visual and audiovisual distraction on pain and anxiety among patients undergoing colonoscopy. *Gastroenterol Nurs*. 2015;38(1):55–61. doi:10.1097/SGA.0000000000000089
53. Zhou XC, Huang YB, Wu S, et al. Lever positioning manipulation alters real-time brain activity in patients with lumbar disc herniation: an amplitude of low-frequency fluctuation and regional homogeneity study. *Psychiatry Res*. 2023;334:111674. doi:10.1016/j.pscychresns.2023.111674
54. Shi H, Yuan C, Dai Z, Ma H, Sheng L. Gray matter abnormalities associated with fibromyalgia: a meta-analysis of voxel-based morphometric studies. *Semin Arthritis Rheum*. 2016;46(3):330–337. doi:10.1016/j.semarthrit.2016.06.002